Vol. **123** (2013) *ACTA PHYSICA POLONICA A* No. 2

Proceedings of the 2nd International Congress APMAS2012, April 26–29, 2012, Antalya, Turkey

High-Coercivity FePt Nanoparticle Assemblies Embedded in Oxide-Matrix by Atomic Layer Deposition

J.-Z. KONG[a,b], A.-D. LI[a,*], M.-Y. GAO[a], Q.-Y. YAN[c] AND D. WU[a]

[a]Materials Science and Engineering Department, National Laboratory of Solid State Microstructures
Nanjing University, Nanjing 210093, P.R. China

[b]Nanjing University Aeronaut & Astronaut, Academy Frontier Science, Nanjing 210016, P.R. China

[c]School of Materials Science and Engineering, Nanyang Technological University, Singapore 639798

Self-assembled face-centered cubic FePt nanoparticles were embedded into the oxide capping layer using the atomic layer deposition technology. The effect of the oxide-matrix layer on the structure, mono-dispersibility, and magnetic properties of the FePt/oxide composite thin films was investigated. Experimental results suggest that the protection of the oxide-matrix capping layer can effectively inhibit the grain growth and particle aggregation, and preserve the ordered domains of the FePt nanoparticles during the $L1_0$ ordering transition through annealing. The combination of the atomic layer deposition capping layer and self-assembled FePt nanoparticles provides a new potential approach to fabricate the ultrahigh-density magnetic recording media.

DOI: 10.12693/APhysPolA.123.173

PACS: 75.50.Vv, 75.75.Cd, 75.50.Bb, 75.50.Ss

1. Introduction

Chemically $L1_0$-ordered face-centered tetragonal (fct) FePt nanoparticles (NPs) have great application potential in advanced magnetic materials such as ultrahigh-density recording media and high-performance permanent magnets [1–3]. Typically, the phase transition from chemically disordered face-centered cubic (fcc) FePt to fct-FePt occurred at high temperatures annealing [1]. Kang et al. reported that the addition of Ag and/or Au can result in an appreciable reduction of the $L1_0$ phase transition temperature about 100–200 °C [4, 5]. However, the heat-treated temperature above 450 °C may cause aggregation and sintering and decrease the particle positional order. Recently, Yan et al. reported that the temperature of $L1_0$ phase transformation could be lowered to 300 °C by doping Sb, and the ordering is promoted by defects produced by the additives during annealing, because those additives with very low surface energy are easy to segregate, resulting in the difficulty in formation of large-area assembly [6, 7]. In order to overcome above problems, FePt NPs are either annealed by a salt-matrix technique [8], or coated with SiO_2 [9] or MgO [10] to minimize the sintering effects during the $L1_0$-phase transition annealing. Unfortunately, the assembly of FePt NPs is destroyed due to the strong magnetic interaction.

In the present study, we demonstrate a new flexible approach for the preparation of the FePt/oxide-matrix composite thin films. As-prepared FePt NPs were self-assembled on Si(001) substrates by drop-casting, and then a continuous oxide capping layer was deposited onto the assembled FePt particle films by atomic layer deposition technology. During annealing, the oxide-matrix capping layer could maintain the position order of the FePt NPs self-assembly, leading to a durable composite magnetic film with high thermal and chemical stability.

2. Experimental details

Well-separated FePt NPs with particle size of ≈ 4.5 nm were prepared by the chemical reduction of $Pt(acac)_2$ and thermal decomposition of $Fe(CO)_5$ in the presence of oleic acid (OA) and oleylamine (OAm) [9, 11, 12]. Samples for the self-assembled FePt NPs were prepared by drop-casting a drop of FePt dispersion colloid including small amounts of OA and OAm onto the HF-treated Si (001) substrates. The Al_2O_3 and TiO_2 capping layer with various thicknesses were deposited onto the self-assembled FePt particle films at a growth temperature of 200 °C, respectively, using trimethylaluminium (TMA) and Ti isopropoxide (TIP) as metal sources and pure water as oxygen source by atomic layer deposition (ALD) (Picosun SUNALE^{TM} R-150B) to obtain the composite thin films of fcc-FePt NPs/oxide-matrix. Finally, the composite film samples were annealed at 700 °C for 1 h under the flow of forming gas (93% Ar + 7% H_2).

The crystallographic textures of samples were characterized by means of X-ray diffraction (XRD) (D/max 2000, Rigaku) using Cu K_α radiation, and TEM (Tecnai G^2 F20 S-Twin, FEI). The average composition of as-prepared FePt NPs was determined to be $Fe_{52}Pt_{48}$ by the energy dispersive X-ray spectroscopy attached to transmission electron microscopy (TEM), with an error of ±2%. The X-ray photoelectron spectroscopy (XPS) measurements were performed on a Thermo Fisher K-Alpha spectrophotometer with Al K_α radiation. The binding energies were calibrated with respect to the signal from the adventitious carbon (binding energy 284.8 eV). Magnetic hysteresis loops of the annealed sam-

---

[*] corresponding author

ples were measured at the room temperature (RT) with a vibrating sample magnetometer (VSM) integrated in the physical properties measurement system (PPMS-9).

3. Results and discussion

In order to investigate the fcc to fct phase transition, FePt particle/oxide-matrix composite films on Si substrates were annealed at 700 °C under the reductive atmosphere for 1 h. Figure 1 shows the XRD patterns of bare FePt NPs, FePt/TiO_2, and FePt/Al_2O_3 samples. The ordered fct-FePt phases have been formed in three samples, as confirmed by the appearance of the Bragg peaks of (001), (110), (002) and (201). It is easily seen that the bare FePt NPs on Si has strongest peak intensity and narrowest the full width at half maximum (FWHM) of the (111) peak. It indicates obvious grain growth and severe aggregation of FePt NPs without any protection layer. The FePt/Al_2O_3 composite sample exhibits weakest peak intensity and broadest FWHM of the (111) peak, implying that the Al_2O_3-matrix layer (10 nm thick) can effectively prevent the FePt particles from the coalescence and sintering during annealing at 700 °C. Using the Sherrer equation, the average sizes of FePt NPs are calculated to be 14.9, 5.9, and 10.4 nm in bare FePt NPs, FePt/Al_2O_3, and FePt/TiO_2, respectively. Why does the TiO_2 capping layer show relatively poorer impact on preventing from aggregation, in comparison with Al_2O_3 capping layer? The main reason lies in various precursor chemistry mechanisms of TMA and TIP during ALD growth, leading to large difference in deposition rate of Al_2O_3 and TiO_2. ALD of Al_2O_3 using TMA and H_2O as precursors follows complete ideal self-limiting surface chemisorption reaction with 0.1 nm/cycle, whereas ALD of TiO_2 using TIP and H_2O is nonideal ALD behavior with slower rate of 0.02–0.03 nm/cycle. Under similar ALD processing condition of 100 cycles, the thickness of TiO_2 capping layer is only about 2–3 nm instead of 10 nm of Al_2O_3 layer. Such ultrathin oxide capping layer can hardly completely isolate FePt NPs ($\approx$ 4.5 nm) and furthermore keep the self-assemble FePt array during annealing.

The XPS analyses were used to characterize the surface composition of the annealed FePt/Al_2O_3 composite films. In Fig. 2a, a symmetric O 1*s* peak located at 531.2 eV appears, indicating only one kind of O species (Al–O bond) exists. This binding energy can be ascribed to the O^{2-} ions in Al_2O_3 lattice. In Fig. 2b, the XPS spectrum at 70–76 eV can be deconvoluted into three peaks from Al 2*p*, Pt $4f_{5/2}$ and Pt $4f_{7/2}$ using Gauss–Lorentzian fitting. The symmetric peak centered at 119.4 eV is attributed to Al 2*s*, as indicated by the inset in Fig. 2b. Due to the limitation of resolution and signal sensitive factor, Fe signal cannot be observed. However, based on the XPS spectra of O 1*s*, Al 2*p*, Pt 4*f* and Al 2*s* and above XRD results, we can deduce the existence of FePt NPs covered with Al_2O_3 thin film.

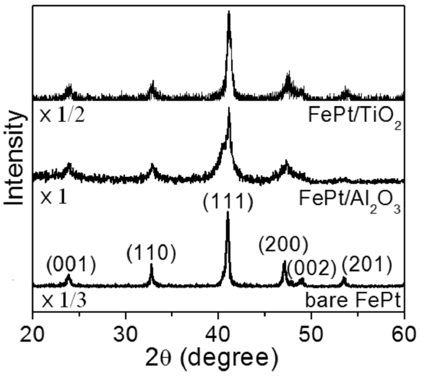

Fig. 1. XRD patterns of the annealed samples of FePt/TiO_2, FePt/Al_2O_3, and bare FePt NPs on Si.

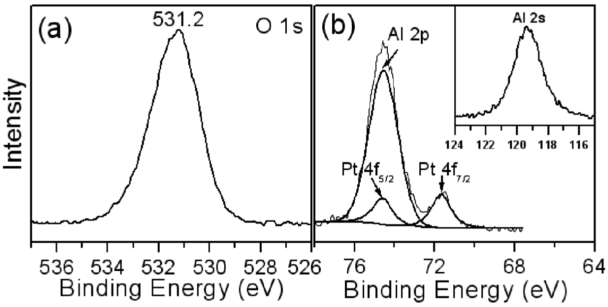

Fig. 2. XPS spectra of the annealed FePt/Al_2O_3 film: (a) O 1*s*; (b) Al 2*p*. Inset (b) shows the corresponding Al 2*s* spectrum.

Sample of the as-prepared FePt NPs was shown in Fig. 3a. This TEM image shows a self-assembled array of well-separated, uniform FePt NPs with the diameter about 4.5 nm, and hexagonal-closed-packed (hcp) monolayer lattice patterns can be identified easily. After 700 °C anneal, large particles (Fig. 3b) with broader size distribution can be found on sample of bare FePt NPs on Si without any protective layer because of the sintering and aggregation among the particles during the $L1_0$ phase transition. Compared with Fig. 3b, the annealed FePt/10 nm thick Al_2O_3 composite films show well-monodispersed FePt NPs embedded in the amorphous Al_2O_3-matrix layer. It means that 10 nm thick Al_2O_3 capping layer is thick enough to effectively prevent the particles from the coalescence and sintering during annealing. Figure 3d plots the particle size and ordering parameter S of FePt in the annealed Al_2O_3 films as a function of the thickness of the capping layer. When the thickness of the capping layer of Al_2O_3 is 5 nm, the particle size is larger than 5 nm due to small amount of aggregation of FePt NPs. When the thickness of the Al_2O_3 capping layer increases to 15 and 20 nm, the average particle sizes keep almost constant in FePt/Al_2O_3 composite films. In addition, with the increase of the capping layer, the long-range S values [6] decrease, which is attributed to the smaller FePt particles embedded in the Al_2O_3-matrix (the particle size effect [13]) and the residual strain at the interfaces. The excessive matrix layer would hinder the $L1_0$ phase transition [10] and decrease the ordering parameter. So, taking into account the trade-off in $L1_0$ phase transition and particle dispersion, the 10 nm thick Al_2O_3 capping layer is considered as the optimal thickness for magnetic recording applications.

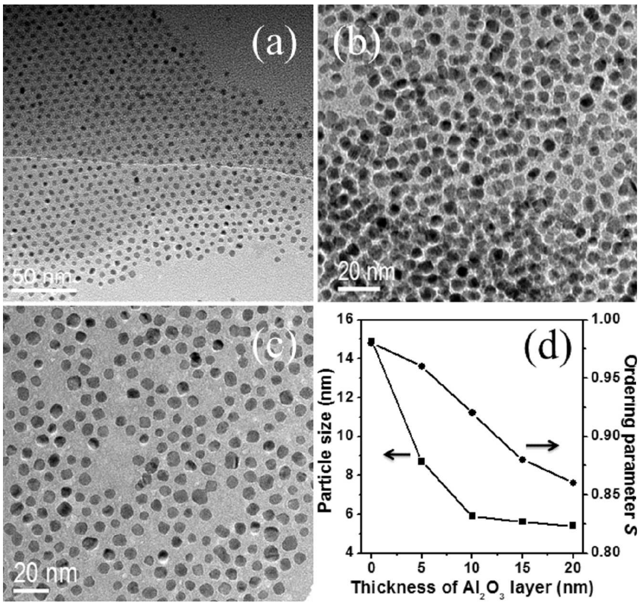

Fig. 3. (a) TEM image of as-prepared FePt NPs; (b) and (c) TEM images of FePt NPs on Si substrates after annealing at 700 °C for 1 h: (b) without Al_2O_3 protection layer, (c) with 10 nm thick Al_2O_3 capping layer; (d) plot of the particle size and ordering parameter S of FePt/Al_2O_3 composite films as a function of the thickness of the capping layer.

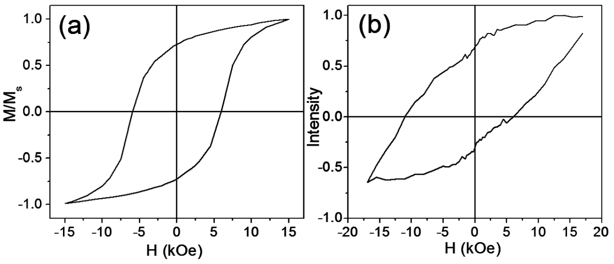

Fig. 4. Room-temperature hysteresis loops of the annealed composite films: (a) FePt/Al_2O_3, and (b) FePt/TiO_2.

Vibrating sample magnetometer (VSM) measurements were performed for the annealed FePt/oxide-matrices. Figure 4a and b shows the hysteresis loop of the heat-treated FePt/10 nm thick Al_2O_3 and FePt/2–3 nm thick TiO_2 composite thin films on Si. As expected, the FePt/Al_2O_3 and FePt/TiO_2 composite thin films successfully transforms from superparamagnetic to ferromagnetic phase after 700 °C annealing with larger coercivity (H_C) of 5.9 kOe and 8.5 kOe, respectively. The FePt/Al_2O_3 sample displays saturated M–H shape with better symmetry whereas the FePt/TiO_2 has unsaturated, asymmetric and unclose loop. This implies that very high anisotropy regions in FePt/TiO_2 cannot be switched at the maximum field of 15 kOe. From the XRD pattern, the average grain size of FePt NPs coated with 2–3 nm thick TiO_2 layer is ≈ 10.4 nm, much larger than ≈ 5.9 nm for the 10 nm thick Al_2O_3 layer. It is well known that the grain size is a key factor affecting the magnetic properties and $L1_0$ ordering process [13, 14]. The coercivity of FePt NPs increases rapidly with the particle size. So it is easily understood why the FePt/TiO_2 composite films have higher H_C than FePt/Al_2O_3. This is related to the larger FePt NPs in TiO_2-matrix due to the sintering and aggregation during the high-temperature annealing process.

4. Conclusions

In summary, we developed a new approach to fabricate the FePt/oxide-matrix composite films by the combination of self-assembly FePt NPs and ALD technology. Self-assembled fcc-FePt NPs on Si were embedded into the ALD-derived oxide capping layer such as Al_2O_3 and TiO_2. It is found that the 10 nm thick Al_2O_3 layer deposited by ALD can prevent FePt NPs from sintering and keep the position order of the FePt NPs assembly with well dispersion and high coercivity. In the future, combining with the FePt NPs self-assembly and *in situ* applied magnetic field during Al_2O_3 ALD deposition, the crystallographic oriented fct-FePt particle arrays would be explored. It will give a new potential approach to fabricate the ultrahigh-density magnetic recording media.

Acknowledgments

This project was supported by the Natural Science Foundation of China (10974085 and 50932001), a grant from the State Key Program for Basic Research of China (20120091110049, 2011CB922104, and 2009CB929500) and the Fundamental Research Funds for the Central Universities. Aidong Li also thanks the support of PAPD in Jiangsu Province and SRF for ROCS, SEM.

References

[1] S.H. Sun, C.B. Murray, D. Weller, L. Folks, A. Moser, *Science* **287**, 1989 (2000).

[2] H. Zeng, J. Li, J.P. Liu, Z.L. Wang, S.H. Sun, *Nature* **420**, 395 (2002).

[3] S.H. Sun, *Adv. Mater.* **18**, 393 (2006).

[4] S.S. Kang, J.W. Harrell, D.E. Nikles, *Nano Lett.* **2**, 1033 (2002).

[5] V. Tzitzios, D. Niarchos, G. Hadjipanayis, E. Devlin, D. Petridis, *Adv. Mater.* **17**, 2188 (2005).

[6] Q. Yan, T. Kim, A. Purkayastha, P.G. Ganesan, M. Shima, G. Ramanath, *Adv. Mater.* **17**, 2233 (2005).

[7] Q. Yan, T. Kim, A. Purkayastha, Y. Xu, M. Shima, R.J. Gambino, G. Ramanath, *J. Appl. Phys.* **99**, 08N709 (2006).

[8] C.B. Rong, D. Li, N. Poudyal, V. Nandwana, N. Poudyal, Y. Ding, Z.L. Wang, H. Zeng, J.P. Liu, *Adv. Mater.* **18**, 2984 (2006).

[9] Q. Yan, A. Purkayastha, A.P. Singh, H. Li, A.D. Li, R.V. Ramanujan, G. Ramanath, *Nanotechnology* **20**, 025609 (2009).

[10] A. Tomou, I. Panagiotopoulos, D. Gournis, B. Kooi, *J. Appl. Phys.* **102**, 023910 (2007).

[11] J.Z. Kong, Y.P. Gong, X.F. Li, A.D. Li, J.L. Zhang, Q.Y. Yan, D. Wu, 10.1039/c0jm03268a*J. Mater. Chem.* **21**, 5046 (2011).

[12] J.L. Zhang, J.Z. Kong, A.D. Li, Q.Y. Yan, D. Wu, *J. Sol-Gel Sci. Tech.* **64**, 269 (2012).

[13] Y. Ding, S.A. Majetich, *Appl. Phys. Lett.* **87**, 022508 (2005).

[14] Y. Ding, D. Farrell, S. Yamamuro, S.A. Majetich, *J. Appl. Phys.* **93**, 7411 (2003).